ACS chemical biology

Letters

pubs.acs.org/acschemicalbiology

Modular Isotopomer Synthesis of γ-Hydroxybutyric Acid for a Quantitative Analysis of Metabolic Fates

Sushabhan Sadhukhan,[†,§] Guo-Fang Zhang,*[,‡] and Gregory P. Tochtrop*[,†]

Departments of [†]Chemistry and [‡]Nutrition, Case Western Reserve University, 10900 Euclid Avenue, Cleveland, Ohio 44106, United States

Supporting Information

ABSTRACT: Herein we report a study combining metabolomics and mass isotopomer analysis used for investigation of the biochemical fate of γ-hydroxybutyric acid (GHB). Using various ^{13}C incorporation labeling patterns into GHB, we have discovered that GHB is catabolized by previously unknown processes that include (i) direct β-oxidation to acetyl-CoA and glycolate, (ii) α-oxidation to 3-hydroxypropionyl-CoA and formate, and (iii) cleavage of C-4 to yield 3-hydroxypropionate and CO_2. We further utilized the unique attributes of our labeling patterns and the resultant isotopomers to quantitate relative flux down the identified pathways.

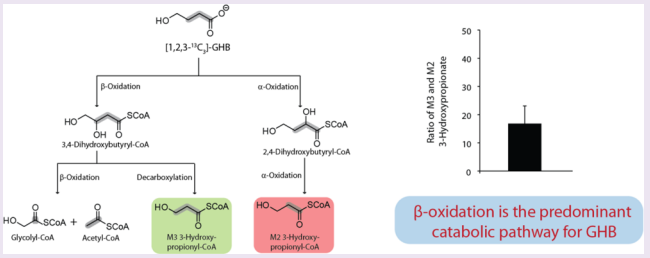

γ-Hydroxybutyric acid (GHB) is a ubiquitous molecule in vivo, derived both endogenously (from the metabolism of the neurotransmitter γ-aminobutyric acid, GABA)[1,2] and exogenously in the form of a drug of abuse or prescription medication (sodium oxybate).[3] Recently, we reported two novel catabolic pathways, which act in parallel to effectively recycle 4-hydroxyacids to the fundamental cellular building blocks of acetyl-CoA, propionyl-CoA, and formate.[4,5] The hallmark of these newly discovered pathways involves the phosphorylation and subsequent isomerization of 4-hydroxyacyl-CoAs to molecules that can readily be catabolized via β-oxidation. An interesting caveat of this work was that GHB did not generally proceed down the identified pathways. Rather, 4-phosphobutyryl-CoA is found in very low concentration and generally undergoes further β-oxidation processes to form smaller cellular building blocks such as acetyl-CoA.

An analysis of the literature reveals only one defined pathway for the catabolism of GHB in vivo comprising its conversion to succinic semialdehyde and subsequent oxidation to succinate, an intermediate of the citric acid cycle.[6,7] However, during our investigations we discovered that this anaplerosis,[8,9] which is defined as the contribution of GHB to the catalytic intermediates of the citric acid cycle, represented only 8% of the steady-state fate of GHB. To develop a more thorough understanding of GHB metabolism, we initiated a comprehensive metabolomics study using the chemical synthesis of different GHB isotopomers and rat liver perfusion that enabled us to show that in addition to the metabolic fates described above, GHB is also catabolized by processes that include (i) direct β-oxidation resulting in acetyl-CoA and glycolate, (ii) production of 3-hydroxypropionyl-CoA and formate via an α-oxidation step, and (iii) cleavage of C-4 via an as of yet undetermined mechanism to yield 3-hydroxypropionate and carbon dioxide (Figure 1).[10] Although these findings represent a major step forward in understanding the fate(s) of GHB in vivo, a central question still remained as to the relative contributions of the various pathways to the ultimate fate of GHB.

In the present work, we have developed a series of analytical tools that allow for a quantitative analysis of the steady state metabolic fates for GHB. The relevance of these tools and studies herein are multifaceted but can be clearly illustrated by a rare inborn error in metabolism whereby individuals who lack the ability to convert GHB to succinic semialdehyde (succinic semialdehyde dehydrogenase deficiency or GHB aciduria) present clinically with developmental delay, mental retardation, and seizure.[11,12] This combined with the greatly expanded use of GHB clinically illustrate the relevance of defining a comprehensive understanding of the fate(s) of this molecules.

As stated above, we have established that β-oxidation and α-oxidation processes play critical roles in GHB metabolism.[10] While β-oxidation reactions have been extensively studied for different biological transformations, little is known about α-oxidation processes. Fatty acid α-oxidations are generally characterized by identifying the labeled formate or formyl-CoA production from the carboxy terminal, but the observation of ^{13}C-labeled formate (M1 formate) is not sufficient to conclude that the putative α-oxidation occurs as M1 formate may arise from oxidation of glycine, serine, glycolate, and 3-phospho-glycerate if these compounds become ^{13}C-labeled from the labeled parent molecules.[13] One of the goals of the current study was to develop a simple and sensitive method to define α-oxidation via precursor-to-product relationships and

Received: April 23, 2013
Accepted: June 16, 2014
Published: June 16, 2014

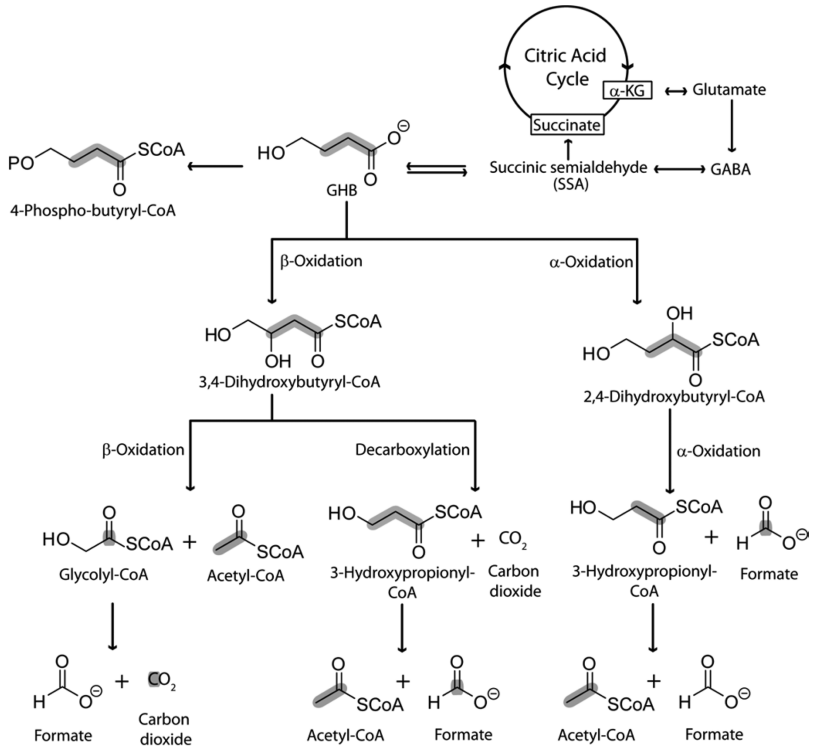

Figure 1. GHB catabolism via different processes demonstrated by using [1,2,3-$^{13}C_3$]-GHB.

Scheme 1. Synthetic Strategy for the Labeled GHB Molecules; ^{13}C Labels Are Shown with the Colored Asterisks (∗)

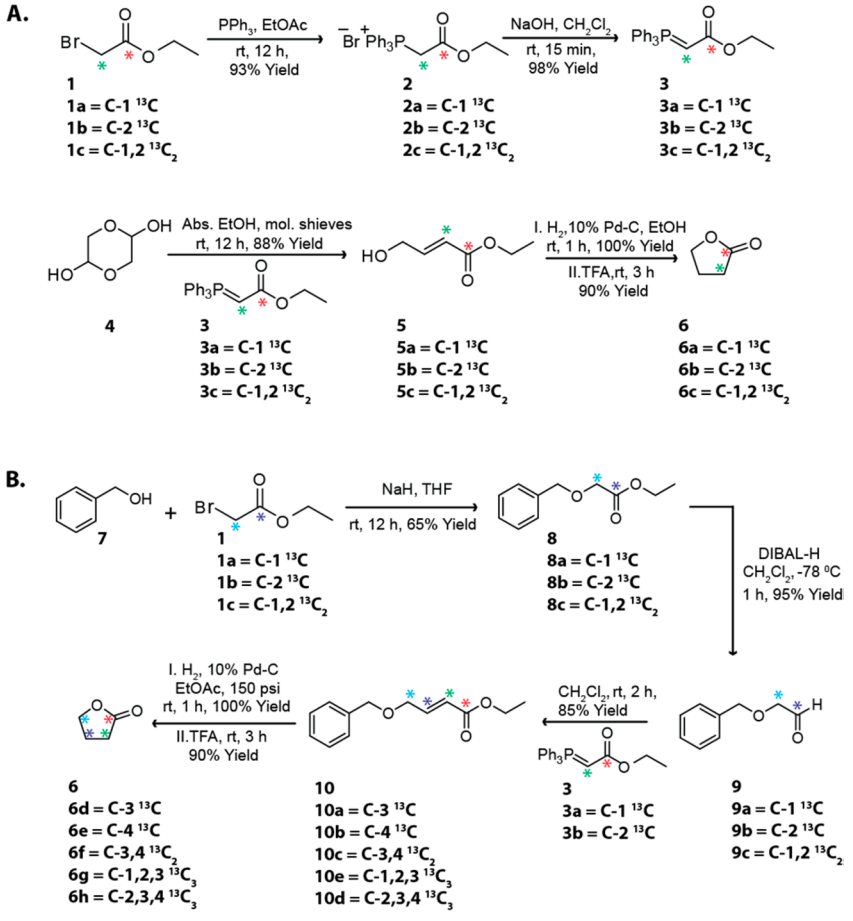

dx.doi.org/10.1021/cb500380b | ACS Chem. Biol. 2014, 9, 1706−1711

measure its rate versus the competitive β-oxidation step for GHB metabolism. Essential to this work was the strategic synthesis of isotopically labeled GHB molecules and evaluation of the mass isotopomer distributions of its metabolites.

Our first challenge was to devise synthetic route(s) that would be high-yielding and efficient but more importantly would allow the incorporation of ^{13}C at any permutation of carbons. While GHB syntheses have been reported previously, none would allow for the criteria above.[14] As shown in Scheme 1, we developed two separate routes for the incorporation of ^{13}C labels at any position(s) of γ-butyrolactone. The rationale behind two different synthetic routes was based on the fact that despite Scheme 1A being very high-yielding, it can only incorporate ^{13}C label selectively at C-1 or C-2 or C-1,2. Therefore, to achieve labeling permutations that include C-3 and/or C-4, another strategy was developed as outlined in Scheme 1B. To illustrate Scheme 1A, we show the synthesis of [1,2-$^{13}C_2$]-γ-butyrolactone (**6c**) starting from glycoaldehyde dimer (**4**), which serves as a convenient in situ source of 2-hydroxyacetaldehyde.[15,16] The Wittig olefiniation followed by hydrogenation and acid-catalyzed lactonization afforded [1,2-$^{13}C_2$]-γ-butyrolactone, **6c**, in 75% overall yield. In this case, the labeling can be controlled through the Wittig reagent, **3c**, which was synthesized from commercially available labeled ethyl bromoacetate (**1c**) depending upon the desired labeling. In Scheme 1B we illustrate the example of [1,2,3-$^{13}C_3$]-γ-butyrolactone (**6g**), synthesized starting with ethyl-[1-^{13}C]-2-bromoacetate (**1a**), which was reacted with the sodium salt of benzyl alcohol followed by DIBAL-H reduction to give the α-(benzyloxy)-[1-^{13}C]-acetaldehyde (**9a**). This was subsequently subjected to Wittig olefination using ^{13}C-labeled Wittig reagent (**3c**) followed by hydrogenation and acid-catalyzed lactonization as above to afford the [1,2,3-$^{13}C_3$]-γ-butyrolactone, **6g**, with the overall yield of 55%. Storage of GHB in the lactone form ameliorates issues of autolactonization that occurs during long-term storage.

Our experimental system for studying the metabolism of GHB is via perfusion of live rat liver, which has been reported previously.[17] This approach allows us to work in a carefully controlled experimental setup while still using primary tissues (mimicking in vivo conditions) as compared to transformed and immortalized cell culture lines where we could not be sure of the physiologic relevance.

We first sought to quantitatively measure the first divergent step where either 3,4- or 2,4-dihydroxybutyryl-CoA is produced via β-oxidation and α-oxidation, respectively; see Figure 1. To confirm their production, we conducted an experiment with [1,2,3,4-$^{13}C_4$]-GHB (M4 GHB) and subsequently identified M4 labeling in both dihydroxybutyrates. An interesting observation of this experiment was that although we found extensive M4 labeling on 2,4-dihydroxybutyrate, the 3,4-dihydroxybutyrate was labeled as both M2 and M4. Further experiments with [1,2-$^{13}C_2$]- and [3,4-$^{13}C_2$]-GHB revealed that the C-1 and C-2 of 3,4-dihydroxybutyryl-CoA readily equilibrate with endogenously present acetyl-CoA (unlabeled) from other sources. We attribute the equilibration to two reverse reactions catalyzed by 3-hydroxyacyl-CoA dehydrogenase and 3-ketoacyl-CoA thiolase. This finding illustrates the inherent value in being able to produce GHB with any permutation of carbon labeling, as [1-^{13}C]-, [2-^{13}C]-, or [1,2-$^{13}C_2$]-GHB would not accurately differentiate the initial flux of β-oxidation versus α-oxidation. Our initial attempts to quantitate relative fluxes centered on an analysis of relative abundance of 3,4- and 2,4-dihydroxybutyryl-CoA. However, after it was determined that absolute rates of flux could not specifically be determined for the different molecules, we focused on the common intermediate 3-hydroxypropionyl-CoA. This molecule is common to both the α-oxidation and β-oxidation legs of the pathway, and with the utilization of the [1,2,3-$^{13}C_2$]-GHB and given the steady state nature of the experiments, we can specifically determine relative fluxes by comparing the amount of M3 3-hydroxypropionyl-CoA to M2 3-hydroxypropionyl-CoA (see Figures 1 and 3). The only limitation of this approach is that it can only set a lower boundary (i.e., the ratio is at least the reported value). This limitation became moot upon the analysis of the new data, which showed that the β-oxidation leg of the pathway is at least 16.8 times more predominant as compared to the α-oxidation leg (Figure 3).

Next we aimed to investigate and quantitate the further catabolism of 2,4- and 3,4-dihydroxybutyrates utilizing [1,2,3-$^{13}C_3$]-GHB and [2,3,4-$^{13}C_3$]-GHB. To confirm the fate of C-1, we first perfused rat livers with [1,2,3-$^{13}C_3$]-GHB and found M2 3-hydroxypropionate (from 3-hydroxypropionyl-CoA) and M1 formate, a product we tentatively ascribed to an α-oxidation event. We subsequently found M3 GHB-CoA, M3 2,4-dihydroxybutyrate, M2 3-hydroxypropionate (from the in situ hydrolysis of the CoA esters), and M1 formate in clear precursor-to-product relationship (Figure 2A), This allowed us

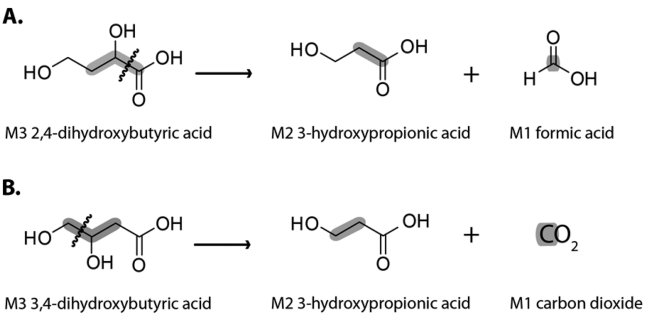

Figure 2. Precursor-to-product relationship from (A) [1,2,3-$^{13}C_3$]-GHB and (B) [2,3,4-$^{13}C_3$]-GHB perfused liver.

to confirm the α-oxidation process. As in other α-oxidation reactions, the sequence involves the hydroxylation on the α-carbon of GHB-CoA forming 2,4-dihydroxybutyryl-CoA, followed by its catabolism to give 3-hydroxypropionyl-CoA, and formyl-CoA, which spontaneously converts to formate during analysis. To uncover the downstream metabolism of 3,4-dihydroxybutyryl-CoA, we conducted experiments with [2,3,4-$^{13}C_3$]-GHB. With this labeling strategy, we predicted M2 glycolyl-CoA, M1 acetyl-CoA, M2 3-hydroxypropionyl-CoA, and M1 formate. This was subsequently confirmed via GC−MS. Further, the identification of glycolate and acetyl-CoA from 3,4-dihydroxybutyryl-CoA confirmed β-oxidation processes in the course of GHB metabolism, which was previously unknown. Additionally, the M2 glycolyl-CoA can be catabolized into M1 formate and CO_2 via glyoxylate (Supplementary Figure 1).

We subsequently applied the precursor-to-product strategy to identify the process(es) leading to formate production from the 3,4-dihydroxybutyryl-CoA. In the [2,3,4-$^{13}C_3$]-GHB perfused liver, we identified M3 GHB-CoA, M3 3,4-dihydroxybutyryl-CoA, M2 3-hydroxypropionyl-CoA, and M1 formate, which are in clear precursor-to-product relationship

dx.doi.org/10.1021/cb500380b | ACS Chem. Biol. 2014, 9, 1706−1711

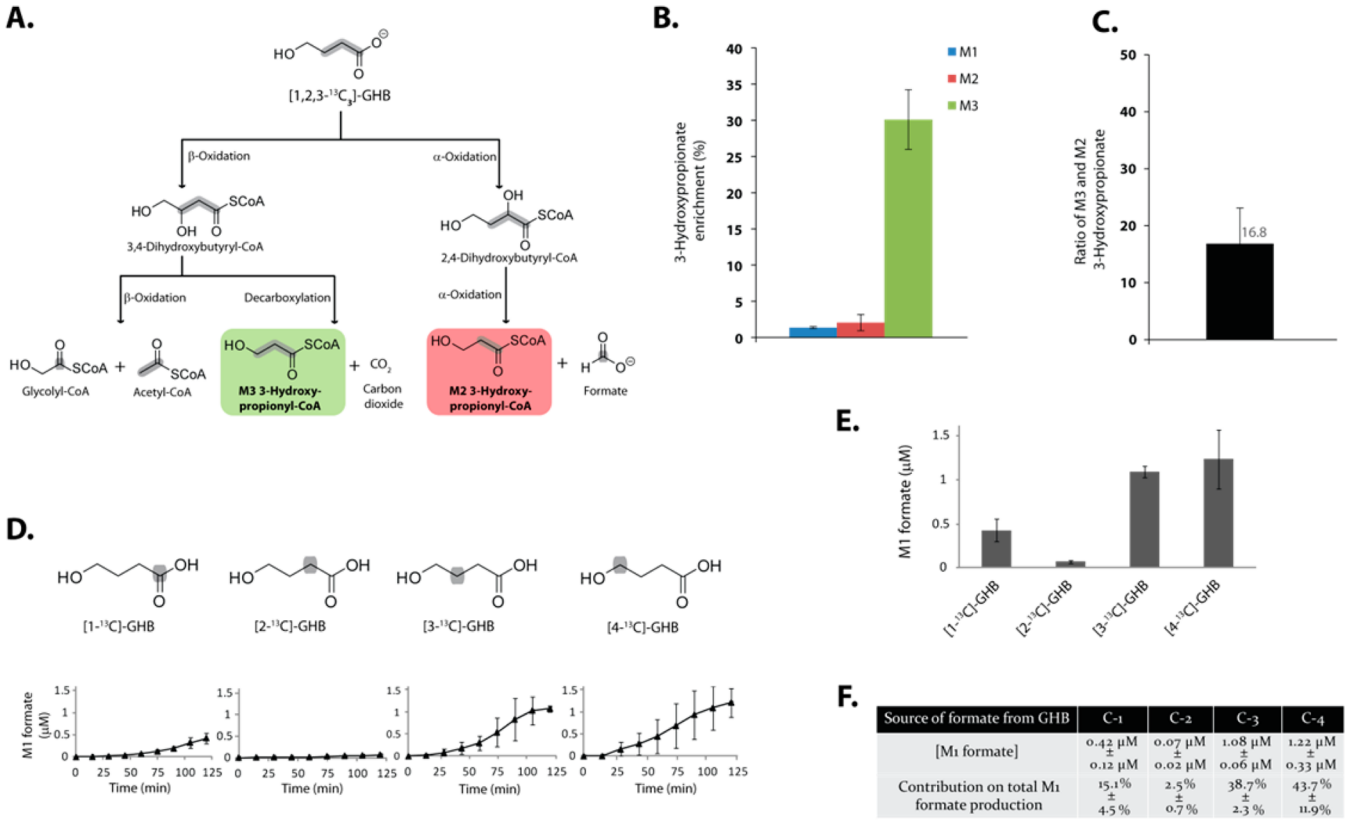

F.

Source of formate from GHB	C-1	C-2	C-3	C-4
[M1 formate]	0.42 μM ± 0.12 μM	0.07 μM ± 0.02 μM	1.08 μM ± 0.06 μM	1.22 μM ± 0.33 μM
Contribution on total M1 formate production	15.1% ± 4.5%	2.5% ± 0.7%	38.7% ± 2.3%	43.7% ± 11.9%

Figure 3. (A) Formation of M3 and M2 3-hydroxypropionyl-CoA from [1,2,3-$^{13}C_3$]-GHB perfusion. (B) 3-Hydroxypropionate enrichment assay in the perfusate from [1,2,3-$^{13}C_3$]-GHB perfused livers. (C) Ratio of M3 3-hydroxypropionate and M2 3-hydroxypropionate enrichment from [1,2,3-$^{13}C_3$]-GHB liver perfusion. (D) M1 formate production from singly labeled GHB perfused liver. (E) Concentration of M1 formate from singly labeled GHB perfused liver after 120 min. (F) Contribution of formate production from different carbon sources. All the perfusions were done in triplicate, and the errors represent standard deviation.

(Figure 2B). However, as this process involves an intermediate of β-oxidation (3,4-dihydroxybutyryl-CoA), we are hesitant to designate it as α-oxidation. Alternatively, the removal of C-4 might involve the oxidation of the primary alcohol into a carboxyl-CoA, followed by its spontaneous removal as CO_2. In this case, the product will be ^{13}C-labeled CO_2, but as we use a large amount of unlabeled CO_2 in our perfusion experiments, it is practically impossible to account for the extent of labeling in the released labeled CO_2.

Using the above logic, we sought to identify a unifying set of experiments that would allow us to confirm our assertion that β-oxidation predominates over α-oxidation as indicated by our 3-hydroxypropionate experiments and also gain further insight into the relative fluxes of the downstream steps. Given that the implications of all of the described pathways impact formate production, we chose to use this as a tool to further assess the quantitative nature of the GHB catabolism. To identify the specific locations of GHB molecule-producing formate and to quantitate the flux down the various pathways, we synthesized singly labeled GHBs ([1-^{13}C]-, [2-^{13}C]-, [3-^{13}C]-, [4-^{13}C]-GHB) and subsequently assayed the M1 formate released from perfused livers as pentafluorobenzyl derivatives under negative chemical ionization to minimize natural enrichment of the analytes (Figure 3).

As shown in Figure 1, M1 formate primarily originates from C-1, C-3, and C-4 of GHB. The formate production from C-1 is derived from the α-oxidation of 2,4-dihydroxybutyryl-CoA as detailed above. The fate of 3,4-dihydroxybutyryl-CoA could undergo either the β-oxidation or decarboxylation reactions to be further metabolized. In the case of β-oxidation, 3,4-dihydroxybutyryl-CoA loses one molecule of acetyl-CoA to produce glycolyl-CoA that can be catabolized to produce formate from its α-carbon.[13] This predominantly accounts for the production of formate from C-4. We attribute the production of labeled formate from C-3 as the result of the cleavage of the β-carbon of 3-hydroxypropionate, which we hypothesize involves a spontaneous retro-aldol type of reaction (Supplementary Figure 2). This reaction would liberate formaldehyde, which would be rapidly converted to formate in vivo. If this hypothesis were true, we would also predict analogous processes from the 3-hydroxypropionate produced from the initial α-oxidation step. Indeed, we observe that formate derived from C-4 represents the largest contribution to the formate pool, which would be congruent with this hypothesis. Current experimentation is underway in the laboratory to definitively define mechanistic fates of 3-hydroxypropionate. Regardless, we postulate that the final fate of C-4 of GHB as formate can mainly be ascribed as the consequence of the catabolism of glycolyl-CoA. The minimal amount of M1 formate from C-2 of GHB likely derives from the nonspecific anaplerotic incorporation of the ^{13}C label during its metabolism in the TCA cycle. Taken together, the results from the analysis of formate production are consistent with the results from the 3-hydroxypropionyl-CoA experiments above that defined β-oxidation as the dominant leg of the pathway shown in Figure 1.

To place this pathway in a more global perspective, we conducted a series of experiments to parse out the four known

dx.doi.org/10.1021/cb500380b | ACS Chem. Biol. 2014, 9, 1706−1711

fates of GHB: (i) conversion to succinate, (ii) conversion to GABA and (iii) catabolism via phosphorylation and isomerization, and (iv) catabolism via the newly discovered pathways described here. In perfusions with M4 GHB, relative anaplerosis was calculated as the enrichment ratio (M4 succinate)/(M4 GHB), as M4 succinate cannot be formed from recycling of label in the citric acid cycle. In the M4 GHB perfused liver, we identified 8 ± 2% of M4 succinate that subsequently enters into the citric acid cycle and 59 ± 6% of M4 GABA. Unlike the longer chain γ-hydroxyacids,[4] 4-phosphobutyryl-CoA was found in very low amount (<1%). The remaining GHB undergoes the catabolic pathways detailed here via conversion to 3,4-dihydroxybutyryl-CoA and 2,4-dihydroxybutyryl-CoA.

In addition to the long history of GHB as a drug of abuse, this molecule is an orphan drug[18] that has long been used to treat narcolepsy with associated cataplexy (under the name sodium oxybate). Further, it is currently being explored for use as a main-line treatment in a variety of prevalent diseases including fibromyalgia[19−21] and Parkinson's.[22] On this basis, a careful understanding of all the metabolic fates of this molecule and the molecular tools to study these fates become critical, especially in the context of defining contraindications due to metabolic toxicity. Regardless, this study clearly illustrates the power of metabolomics studies coupled with stable isotope incorporation to address biochemical questions relevant to human health.

METHODS

Liver Perfusion Experiments. Livers from overnight-fasted Sprague-Dawley rats were perfused for 2 h with 150 mL of recirculating bicarbonate (15 mM) buffer containing 4% dialyzed bovine serum albumin (fraction V, fatty acid-free, Intergen), 4 mM glucose, ±2 mM GHB (unlabeled or labeled GHB). Livers were quick-frozen at the end of the perfusions and stored in liquid nitrogen for further analysis by LC−MS/MS. We subsequently monitored key metabolic intermediates and their mass isotopomer distributions via LC−MS/MS and GC−MS. The mass isotopomers are designated as M, M1, M2, ..., M*n* where *n* is the number of heavy atoms in the molecule.

LC−MS/MS Method for the Labeling Pattern and Concentration Measurement of Acyl-CoAs. For the concentration and labeling pattern of acyl-CoA esters, powdered frozen liver (~200 mg) was extracted for 1 min with 4 mL of (methanol/water 1:1 containing 5% acetic acid) using a Polytron homogenizer. The supernatant was added to a 3 mL ion exchange cartridge packed with 300 mg of 2-(2-pyridyl)ethyl silica gel (Sigma). The cartridge had been preactivated with 3 mL of methanol, then with 3 mL of extraction buffer. The acyl-CoAs that were trapped on the silica gel cartridge were released with (i) 3 mL of a 1:1 mixture of ammonium formate 50 mM pH 6.3 and methanol (to release the short- and medium-chain acyl-CoAs), then (ii) 3 mL of a 1:3 mixture of ammonium formate 50 mM pH 6.3 and methanol, and (iii) 3 mL of methanol (to release the medium- and long-chain acyl-CoAs). The combined effluent was dried under a stream of nitrogen gas and stored at −80 °C until LC−MS/MS analysis.

After dissolving the acyl-CoAs in 100 μL of buffer A (5% acetonitrile in ammonium formate 100 mM, pH 5.0), 40 μL was injected on a Thermo Electron Hypersil GOLD column (150 × 2.1 mm) protected by a guard column (Hypersil Gold 5 μm, 10 × 2.1 mm) in an Agilent 1100 liquid chromatograph. The chromatogram was developed at 0.2 mL/min (i) for 3 min with 98% buffer A and 2% buffer B (95% acetonitrile in ammonium formate 5 mM, pH 6.3), (ii) from 3 to 25 min with a 2% to 60% gradient of buffer B in buffer A, (iii) from 26 to 31 min with 10% buffer A/90% buffer B, (iv) from 32 to 41 min with a 90% to 2% gradient buffer B in buffer A, and (v) 10 min stabilization with 98% buffer A before the next injection.

The liquid chromatograph was coupled to a 4000 QTrap mass spectrometer (Applied Biosystems, Foster City, CA) operated under positive ionization mode with the following source settings: turbo-ion-spray source at 600 °C under N_2 nebulization at 65 psi, N_2 heater gas at 55 psi, curtain gas at 30 psi, collision-activated dissociation gas pressure held at high, turbo ion-spray voltage at 5,500 V, declustering potential at 90 V, entrance potential at 10 V, collision energy at 50 V, collision cell exit potential at 10 V. The Analyst software (version 1.4.2; Applied Biology) was used for data collection and processing.

GC−MS Assay of Formate via Pentafluorobenzyl Bromide (PFBBr) Derivatization Reaction. The concentrations and labeling of formate was assayed as the pentafluorobenzyl derivatives by NH_3-negative chemical ionization as described below. Sample preparation for formic acid with GC−MS assay is as follows. A 400 μL portion of 100 mM PFBBr in acetone solution was added into 200 μL of perfusate samples or standard aqueous solution without precipitating the protein. The sample was incubated at 60−70 °C for 1 h, and 1 mL of hexane was added after the sample had cooled. The sample was then vortexed for 5 min followed by centrifugation at 300*g* for 1 min, and then 200 μL of upper phase (hexane phase) was transferred to GC vials and prepared for GC−MS injection. All experiments were processed in a laminar flow hood to avoid contamination. Distilled Milli-Q water was used for the preparation of all standard solutions.

Analyses were carried out on an Agilent 5973 mass spectrometer, linked to a model 6890 gas chromatograph equipped with an autosampler, an Agilent OV-225 capillary column (30 m, 0.32 mm inner diameter). The carrier gas was helium (2 mL/min) with a pulse pressure of 40 psi. The injection volume was 1 μL with splitless. The injector temperature was set at 200 °C and the transfer line at 250 °C. The GC temperature program was as follows: start at 100 °C, hold for 1 min, increase by 3 °C/min to 145 °C, followed by 50 °C/min to 300 °C, and hold for 5 min. The ion source and the quadrupole were set at 150 °C. The ammonia pressure was adjusted to optimize peak areas. For each analyte, we monitored the signals at the nominal *m*/*z* (M) and at all detectable naturally labeled mass isotopomers with SIM mode. The *m*/*z* monitored are 45 (M) and 46 (M1) for formate.

GC−MS Assay of GHB and Its Carboxylate Metabolites. For the assay of GHB and its carboxylic acid metabolites, perfusate samples (200 μL) spiked with 0.2 μmol of [$^2H_6$]-GHB as internal standard were deproteinized with 2 mL of acetonitrile. After centrifugation and evaporation under N_2, the residue was allowed to react with 100 μL of trimethylsilyl reagent and heated for 1 h at 60 °C. Then, 2 μL was injected into an Agilent 6890 gas chromatograph linked to a 5973 MSD mass spectrometer. The chromatograph was equipped with a 60 m Varian CP 9017 VF-5 capillary column. The carrier gas was helium (26.8 mL/min), and the injection mode was splitless. The injector temperature was set at 290 °C, and the transfer line was held at 290 °C. The column temperature was increased by 3 °C/min from 50 to 300 °C, where it was held for 10 min. The mass spectrometer was operated under electron impact ionization. The quadrupole and ion source temperatures were 150 and 230 °C, respectively. The mass scan ranged from 50 to 700. The *m*/*z* of M0, M1, M2, and M3 3-hydroxypropionates measured as their TMS derivatives are 219, 220, 221, and 222, respectively. The *m*/*z* of M0, M1, and M2 glycoates (TMS derivative) are 205, 206, and 207, respectively. The *m*/*z* of M0, M1, M2, M3, and M4 dihydroxybutyrate-TMS derivatives (same for 2,4- and 3,4-dihydroxybutyrate) are 321, 322, 323, 324, and 325, respectively.

Calculations and Statistics. Correction of raw mass isotopomer profiles for natural enrichment at each mass was conducted with the CORMAT software.[23]

ASSOCIATED CONTENT

Supporting Information

Synthesis details and compound characterization data. This material is available free of charge via the Internet at http://pubs.acs.org.

AUTHOR INFORMATION

Corresponding Authors

*E-mail: gxz35@case.edu.

*E-mail: tochtrop@case.edu.

Present Address

[§]Department of Chemistry and Chemical Biology, Cornell University, 240 Physical Sciences Building, Ithaca, NY 14853, USA.

Notes

The authors declare no competing financial interest.

ACKNOWLEDGMENTS

This work was supported by grants from the National Cancer Institute CA157735 and NSF grant MCB-084480 to G.P.T.

REFERENCES

(1) Snead Iii, O. C., Furner, R., and Chun Che, L. (1989) In vivo conversion of γ-aminobutyric acid and 1,4-butanediol to γ-hydroxybutyric acid in rat brain: Studies using stable isotopes. *Biochem. Pharmacol. 38*, 4375−4380.

(2) Doherty, J. D., Hattox, S. E., Snead, O. C., and Roth, R. H. (1978) Identification of endogenous gamma-hydroxybutyrate in human and bovine brain and its regional distribution in human, guinea pig and rhesus monkey brain. *J. Pharmacol. Exp. Ther. 207*, 130−139.

(3) Miro O Fau - Nogue, S., Nogue S Fau - Espinosa, G., Espinosa G Fau - To-Figueras, J., To-Figueras J Fau - Sanchez, M., and Sanchez, M. (2002) Trends in illicit drug emergencies: the emerging role of gamma-hydroxybutyrate. *J. Toxicol. Clin. Toxicol. 40*, 129−135.

(4) Zhang, G.-F., Kombu, R. S., Kasumov, T., Han, Y., Sadhukhan, S., Zhang, J., Sayre, L. M., Ray, D., Gibson, K. M., Anderson, V. A., Tochtrop, G. P., and Brunengraber, H. (2009) Catabolism of 4-hydroxyacids and 4-hydroxynonenal via 4-hydroxy-4-phosphoacyl-CoAs. *J. Biol. Chem. 284*, 33521−33534.

(5) Sadhukhan, S., Han, Y., Zhang, G.-F., Brunengraber, H., and Tochtrop, G. P. (2010) Using isotopic tools to dissect and quantitate parallel metabolic pathways. *J. Am. Chem. Soc. 132*, 6309−6311.

(6) Kaufman, E. E., Nelson, T., Miller, D., and Stadlan, N. (1988) Oxidation of γ-hydroxybutyrate to succinic semialdehyde by a mitochondrial pyridine nucleotide-independent enzyme. *J. Neurochem. 51*, 1079−1084.

(7) Kaufman, E. E., and Nelson, T. (1987) Evidence for the participation of a cytosolic $NADP^+$-dependent oxidoreductase in the catabolism of γ-hydroxybutyrate in vivo. *J. Neurochem. 48*, 1935−1941.

(8) Reszko, A. E., Kasumov, T., Pierce, B. A., David, F., Hoppel, C. L., Stanley, W. C., Des Rosiers, C., and Brunengraber, H. (2003) Assessing the reversibility of the anaplerotic reactions of the propionyl-CoA pathway in heart and liver. *J. Biol. Chem 278*, 34959−34965.

(9) Owen, O. E., Kalhan, S. C., and Hanson, R. W. (2002) The key role of anaplerosis and cataplerosis for citric acid cycle function. *J. Biol. Chem. 277*, 30409−30412.

(10) Zhang, G.-F., Sadhukhan, S., Ibarra, R. A., Lauden, S. M., Chuang, C. Y., Sushailo, S., Chatterjee, P., Anderson, V. E., Tochtrop, G. P., and Brunengraber, H. (2012) Metabolism of γ-hydroxybutyrate in perfused rat livers. *Biochem. J. 444*, 333−341.

(11) Jakobs C Fau - Bojasch, M., Bojasch M Fau - Monch, E., Monch E Fau - Rating, D., Rating D Fau - Siemes, H., Siemes H Fau - Hanefeld, F., and Hanefeld, F. (1981) Urinary excretion of gamma-hydroxybutyric acid in a patient with neurological abnormalities. The probability of a new inborn error of metabolism. *Clin. Chim. Acta 111*, 169−178.

(12) Gibson, K. M., Hoffmann, C. F., Hodson, A. K., Bottiglieri, T., and Jakobs, C. (1998) 4-Hydroxybutyric acid and the clinical phenotype of succinic semialdehyde dehydrogenase deficiency, an inborn error of GABA metabolism. *Neuropediatrics 29*, 14−22.

(13) Weinhouse, S., and Friedmann, B. (1952) Study of precursors of formate in the intact rat. *J. Biol. Chem. 197*, 733−740.

(14) Näser, U., Pierik, A. J., Scott, R., Çinkaya, I., Buckel, W., and Golding, B. T. (2005) Synthesis of ^{13}C-labeled γ-hydroxybutyrates for EPR studies with 4-hydroxybutyryl-CoA dehydratase. *Bioorg. Chem. 33*, 53−66.

(15) George, W. O., and Collins, G. C. S. (1971) Nuclear magnetic resonance spectra of glycolaldehyde. *J. Chem. Soc. B*, 1352−1355.

(16) Michelsen, H., and Klaboe, P. (1969) Spectroscopic studies of glycolaldehyde. *J. Mol. Struct. 4*, 293−302.

(17) Brunengraber, H., Boutry, M., and Lowenstein, J. M. (1973) Fatty acid and 3-β-hydroxysterol synthesis in the perfused rat liver. *J. Biol. Chem. 248*, 2656−2669.

(18) Bosch, O. G., Quednow, B. B., Seifritz, E., and Wetter, T. C. (2012) Reconsidering GHB: orphan drug or new model antidepressant? *J. Psychopharmacol. 26*, 618−628.

(19) Russell, I. J., Holman, A. J., Swick, T. J., Alvarez-Horine, S., Wang, Y. G., and Guinta, D. (2011) Sodium oxybate reduces pain, fatigue, and sleep disturbance and improves functionality in fibromyalgia: Results from a 14-week, randomized, double-blind, placebo-controlled study. *PAIN 152*, 1007−1017.

(20) Staud, R. (2011) Sodium oxybate for the treatment of fibromyalgia. *Expert Opin. Pharmacother. 12*, 1789−1798.

(21) Scharf, M. B., Baumann, M., and Berkowitz, D. V. (2003) The effects of sodium oxybate on clinical symptoms and sleep patterns in patients with fibromyalgia. *J. Rheumatol. 30*, 1070−1074.

(22) Ondo, W. G., Perkins, T., Swick, T., Hull, K. L., Jr., Jimenez, J. E., Garris, T. S., and Pardi, D. (2008) Sodium oxybate for excessive daytime sleepiness in parkinson disease: An open-label polysomnographic study. *Arch. Neurol. 65*, 1337−1340.

(23) Fernandez, C. A., Des Rosiers, C., Previs, S. F., David, F., and Brunengraber, H. (1996) Correction of 13C mass isotopomer distributions for natural stable isotope abundance. *J. Mass Spectrom. 31*, 255−262.